



OPEN Semaphorin 3F inhibits breast cancer metastasis by regulating the Akt-mTOR and TGF β signaling pathways via neuropilin-2

Hironao Nakayama^{1,2}✉, Akari Murakami³, Hisayo Nishida-Fukuda⁴, Shinji Fukuda⁴, Erina Matsugi¹, Masako Nakahara¹, Chiaki Kusumoto¹, Yoshiaki Kamei³ & Shigeki Higashiyama^{2,5}✉

Class 3 semaphorins are axon guidance factors implicated in tumor and vascular biology, including invasive activity. Recent studies indicate that semaphorin 3F (SEMA3F) is a potent inhibitor of metastasis; however, its functional role in breast cancer is not fully understood. We found that exogenous SEMA3F inhibited phosphorylation of Akt and mTOR downstream kinase S6K in MDA-MB-231 and MCF7 cells via neuropilin-2 (NRP2) receptor. We also examined the effect of SEMA3F on breast cancer progression *in vivo* allograft model. The mouse 4T1 breast cancer cells or 4T1 cells overexpressing SEMA3F (4T1-SEMA3F) were implanted into mammary fat pads of Balb/c mice. We found that tumor growth was significantly inhibited in 4T1-SEMA3F injected mice compared to controls. Immunostaining revealed a remarkable reduction in the expression of vimentin, a mesenchymal cell marker, in 4T1-SEMA3F tumors. We also observed that mice injected with 4T1-SEMA3F cells had minimal metastasis to the liver and lungs, compared to controls. As a novel feature, SEMA3F suppressed TGF β -induced Smad2 phosphorylation, resulting in the inhibition of cell invasiveness and epithelial-to-mesenchymal transition (EMT) in breast cancer. Consistently, a significant correlation between reduced expression of SEMA3F and poor outcome in patients with breast cancer. We conclude that SEMA3F acts as a dual inhibitor of the Akt-mTOR and TGF β signaling pathways; thus, it has the potential to treat metastatic breast cancer.

Keywords Breast cancer, Semaphorin 3F, Neuropilin-2, Metastasis

Breast cancer is one of the most frequently diagnosed cancers and it is still main cause of cancer death in women worldwide, according to GLOBOCAN 2020¹. Metastatic breast cancer is associated with a poor prognosis. Several signaling proteins and pathways are involved in the metastatic potential of breast cancers. The phosphoinositide 3 kinase (PI3K)-Akt-mammalian target of rapamycin (mTOR) pathway is frequently activated in breast cancer, and is associated with resistance to endocrine therapy, human epidermal growth factor receptor 2 (HER2)-directed therapy and cytotoxic therapy in breast cancer^{2–4}. In addition, these malignant properties are driven by the epithelial-to-mesenchymal transition (EMT) induced by activation of the transforming growth factor (TGF) β signaling pathway^{5,6}. However, despite considerable progress, the signaling events mediating cancer cell invasion and metastasis of breast cancer are still incompletely understood, and therapeutic options for the treatment of metastatic breast cancers remain insufficient. Therefore, a better understanding of the molecular mechanisms underlying metastasis is required to develop more effective treatments for this aggressive type of breast cancer.

Neuropilins (NRP) are transmembrane glycoprotein receptors. The NRP genes, *NRP1* and *NRP2*, share approximately 50% structural homology and similar domain structure. Both NRPs bind two disparate ligands, class 3 semaphorins (SEMA3s) and vascular endothelial growth factors (VEGF), and regulate two diverse

¹Department of Medical Science and Technology, Hiroshima International University, Higashi-hiroshima 739-2695, Hiroshima, Japan. ²Division of Cell Growth and Tumor Regulation, Proteo-Science Center (PROS), Ehime University, Toon 791-0295, Ehime, Japan. ³Breast Center, Ehime University Hospital, Toon 791-0295, Ehime, Japan. ⁴Department of Biochemistry, School of Dentistry, Aichi Gakuin University, Nagoya 464-8650, Aichi, Japan. ⁵Department of Oncogenesis and Growth Regulation, Osaka International Cancer Institute, Chuo-ku, Osaka 541-8567, Japan. ✉email: hironao@hirokoku-u.ac.jp; shigeki@m.ehime-u.ac.jp

systems, neuronal guidance and angiogenesis^{7,8}. In contrast, NRP1 and/or NRP2 expression has been detected in many human tumor cell lines. Increased expression of NRP1 and NRP2 is correlated with poor prognosis in patients with breast cancer^{9,10}. NRPs also interact with several growth factors, including placental growth factor 2 (PlGF2)¹¹, fibroblast growth factor 2 (FGF2)¹², hepatocyte growth factor (HGF)^{13,14}, and TGFβ^{13,15,16}. Therefore, NRPs play crucial roles in tumor progression by promoting aberrant growth factor signaling related to EMT-associated drug resistance and metastasis.

Neuronal networking is regulated by a combination of attractive and repulsive cues, called axon guidance molecules. Semaphorin 3F (SEMA3F), a member of the SEMA3s (SEMA3A to G), is first described as a chemorepulsive factor capable of collapsing axonal growth cones, and regulates axon pathfinding during neuronal development^{17,18}. However, SEMA3F also exhibits non-neuronal properties. Further studies have shown that SEMA3F inhibits the migration of endothelial cells (EC) and tumor cells *in vitro* and tumor progression, metastasis, and angiogenesis *in vivo*^{19,20}. Our laboratory has previously analyzed SEMA3F and NRP2 in several cell types, including glioblastoma cell, EC, and T cell. SEMA3F binds to NRP2 receptor, and subsequently forming complexes with the plexin A family receptors on the cell surface. SEMA3F inactivates RhoA, a small GTPase, leading to depolymerization of F-actin, loss of stress fibers and diminished EC and tumor cell migration²⁰. In addition, SEMA3F inhibits PI3K-Akt-mTOR signaling via interactions with NRP2-Plexin A1 receptors²¹. Therefore, SEMA3F is a secreted physiological mTOR inhibitor for diverse human cell types expressing NRP2, indicating that it has broad biological effects and therapeutic potential for cancer treatment. However, the functional roles of SEMA3F and NRP2 in breast cancer are not fully understood.

In this report, we show that SEMA3F inactivates Akt and mTOR downstream signaling molecules, including S6K, via NRP2 in breast cancer cells, even in phosphatase and tensin homologue deleted on chromosome ten (PTEN) deficient breast cancer cells. We also show that SEMA3F inhibits breast cancer cell invasion through Matrigel-coated Transwells *in vitro* and suppresses metastasis to the liver and lungs *in vivo*. As a novel feature, SEMA3F abrogates TGFβ-induced phosphorylation of Smad2, thereby inhibiting breast cancer cell invasion. In addition, significant alterations in TGFβ-target and EMT-related gene expression were observed in breast cancer cells overexpressing SEMA3F. We conclude that SEMA3F is a dual inhibitor of the Akt-mTOR and TGFβ signaling pathways, indicating its potential for the treatment of aggressive types of breast cancer.

Results

Correlation of expression of SEMA3F with breast cancer patient's survival

To determine whether SEMA3F expression correlates with breast cancer progression, we analyzed the relapse-free survival (RSF) of patients with breast cancer by Kaplan-Meier plotter (Gene chip dataset)^{22,23}. Statistical analysis revealed a significant correlation between reduced expression of SEMA3F and poor global patient's survival (Fig. 1A). We also utilized Kaplan-Meier plots in breast cancer patients obtained from RNA sequencing dataset²⁴, and found that reduced expression of SEMA3F was strongly associated with poor outcome in patients with breast cancer (Fig. 1B). When patients were stratified according to positive or negative lymph node status, reduced SEMA3F expression was significantly associated with shorter RSF in lymph node positive patients, whereas there was no significant difference in lymph node negative patients (Fig. 1C, D). These findings suggested that SEMA3F acts as a tumor suppressor and prompted us to investigate the functional role of SEMA3F in the progression and metastasis of breast cancer.

Exogenous SEMA3F inhibits Akt and S6K phosphorylation and inactivates invasiveness of breast cancer cells

To determine the biological effect of SEMA3F in breast cancer cells, we initially profiled the expression levels of semaphorin receptors NRP1 and NRP2 in three intrinsic subtypes of human breast cancer cell lines: luminal (MCF7 and T47D), HER2 (MDA-MB-453 and SK-BR3), and basal (MDA-MB-231, MDA-MB-436, and BT-549). While NRP1 expression was observed only in MDA-MB-231 cells, NRP2 expression was observed in all the intrinsic subtypes (Fig. 2A). By Western blot analysis, we found that administration of recombinant human SEMA3F protein inhibited Akt and S6K (mTOR downstream signaling) phosphorylation in MCF7 and MDA-MB-231 cells within 30 min (Fig. 2B). We generated NRP2 knockout (CRISPR-NRP2) cells using the NRP2-CRISPR-Cas9 vector in MDA-MB-231 cells. Western blot analysis showed that CRISPR-Cas9-mediated cells lacked NRP2, but not NRP1 expression (Fig. 2C). SEMA3F failed to inhibit Akt and S6K phosphorylation in NRP2 knockout cells (Fig. 2C). SEMA3F also inhibited parental MDA-MB-231 cell invasion in Transwells by 25% (Fig. 2D); however, SEMA3F had no effect on NRP2 knockout cells. Fluorescence microscopy in conjunction with phalloidin staining was used to analyze the effects of SEMA3F on MDA-MB-231 cell morphology and stress fiber formation. SEMA3F inhibited stress fibers by 90% in parental cells (Fig. 2E), whereas it had minimal effects on NRP2 knockout cells. These data suggest that SEMA3F inactivates Akt-mTOR signaling and induces cytoskeletal collapse in breast cancer cells by interacting with NRP2.

SEMA3F inactivates Akt-mTOR signaling and invasiveness in PTEN loss breast cancer cells

Loss of PTEN is implicated in breast cancer progression and resistance to targeted therapies, and promotes tumorigenesis by activating PI3K-Akt signaling^{25,26}. To examine whether PTEN is involved in SEMA3F-mediated inactivation of Akt-mTOR signaling, we generated a PTEN knockout (CRISPR-PTEN) breast cancer cell line using the CRISPR-Cas9 system. Western blot analysis confirmed that CRISPR-Cas9-mediated cells lacked PTEN expression, and showed marked increases in Akt and S6K phosphorylation (Fig. 3A). Treatment with SEMA3F resulted in reduced levels of both Akt and S6K phosphorylation in PTEN knockout cells (Fig. 3A). To confirm these results, PTEN knockout cells were transfected with PTEN expression vector. SEMA3F also inactivated Akt-mTOR signaling in the cells re-expressing or overexpressing PTEN (Supplementary Fig. 1A, B). Moreover, there was no change in NRP2 expression level between parental MDA-MB-231 cells and PTEN

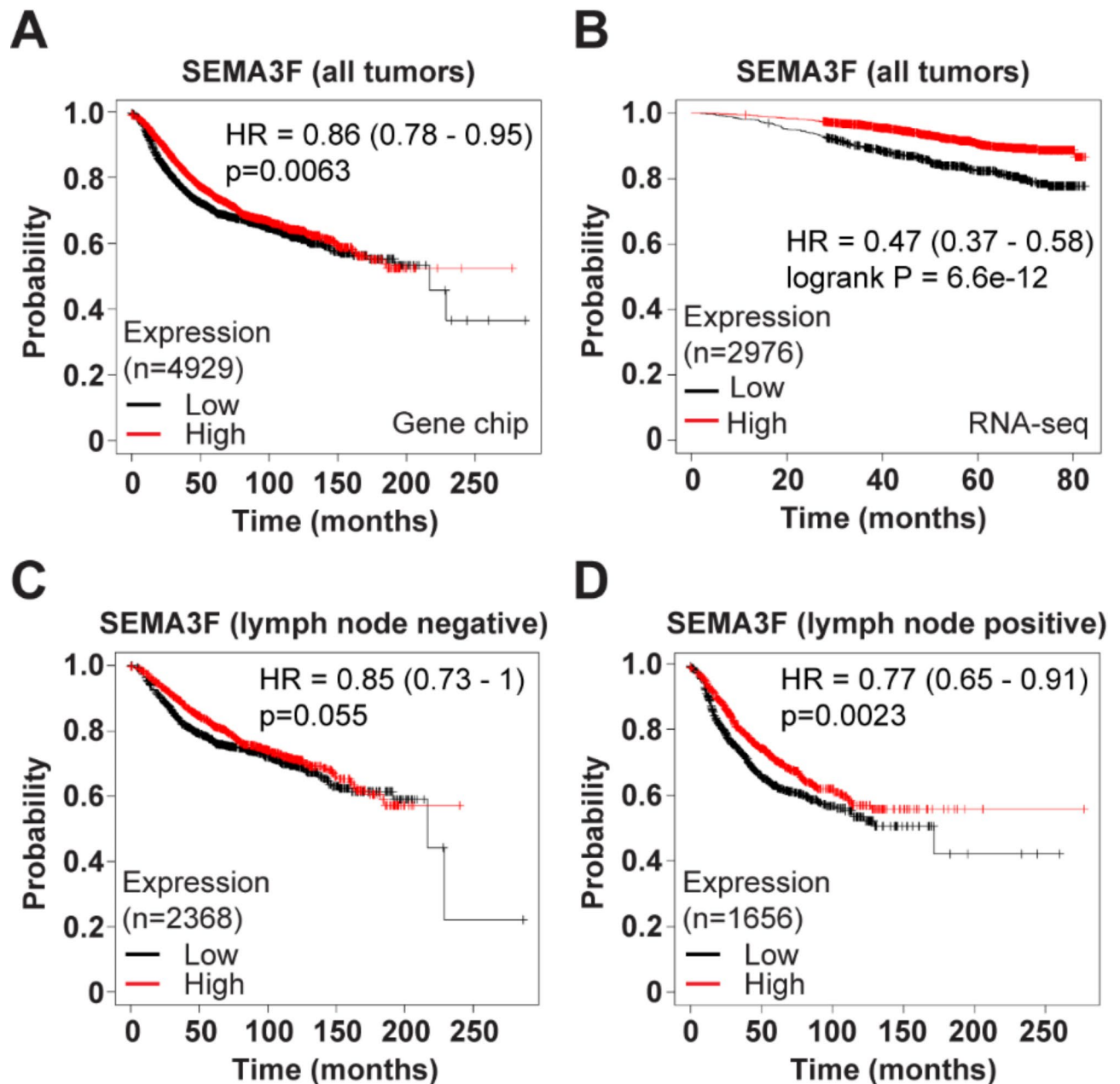


Fig. 1. Correlation of SEMA3F expression with breast cancer patient's survival. (A,B) Kaplan-Meier analysis of relapse-free survival (RSF) of breast cancer patients with low (black) or high (red) SEMA3F mRNA expression by Kaplan-Meier plotter (A Gene chip dataset; B RNA sequencing dataset). (C,D) Kaplan-Meier analysis of RSF of breast cancer patients with low or high SEMA3F mRNA expression, according to negative (C) or positive (D) lymph node status by Kaplan-Meier plotter. Hazard ratios (HR) are included.

knockout cells (Supplementary Fig. 1C). Additionally, the Transwell invasion assay showed that SEMA3F inhibited cell invasion, even in PTEN knockout cells (Fig. 3B). These results suggest that SEMA3F elicits its regulatory response via PTEN-independent mechanisms as we have previously shown in glioblastoma cells²¹.

SEMA3F inhibits breast cancer growth, angiogenesis, and metastasis *in vivo*

To determine the *in vivo* relevance of our signaling studies, we evaluated the effect of SEMA3F on tumor growth in a well-established allograft model, using the mouse mammary tumor cell line 4T1. The 4T1-Control (empty vector) cells or 4T1 cells engineered to constitutively overexpress human SEMA3F-V5 (4T1-SEMA3F) were prepared (Fig. 4A). Each cell line was implanted into the mammary fat pads of Balb/c mice (1×10^6 /mouse); and tumor size (mm^3) was measured at the indicated time points over a period of 24 days. We found that primary tumor growth and weight were significantly suppressed when SEMA3F-producing cells were implanted, compared to controls (Fig. 4B, C). To confirm this observation, tumors were removed and immunostaining was

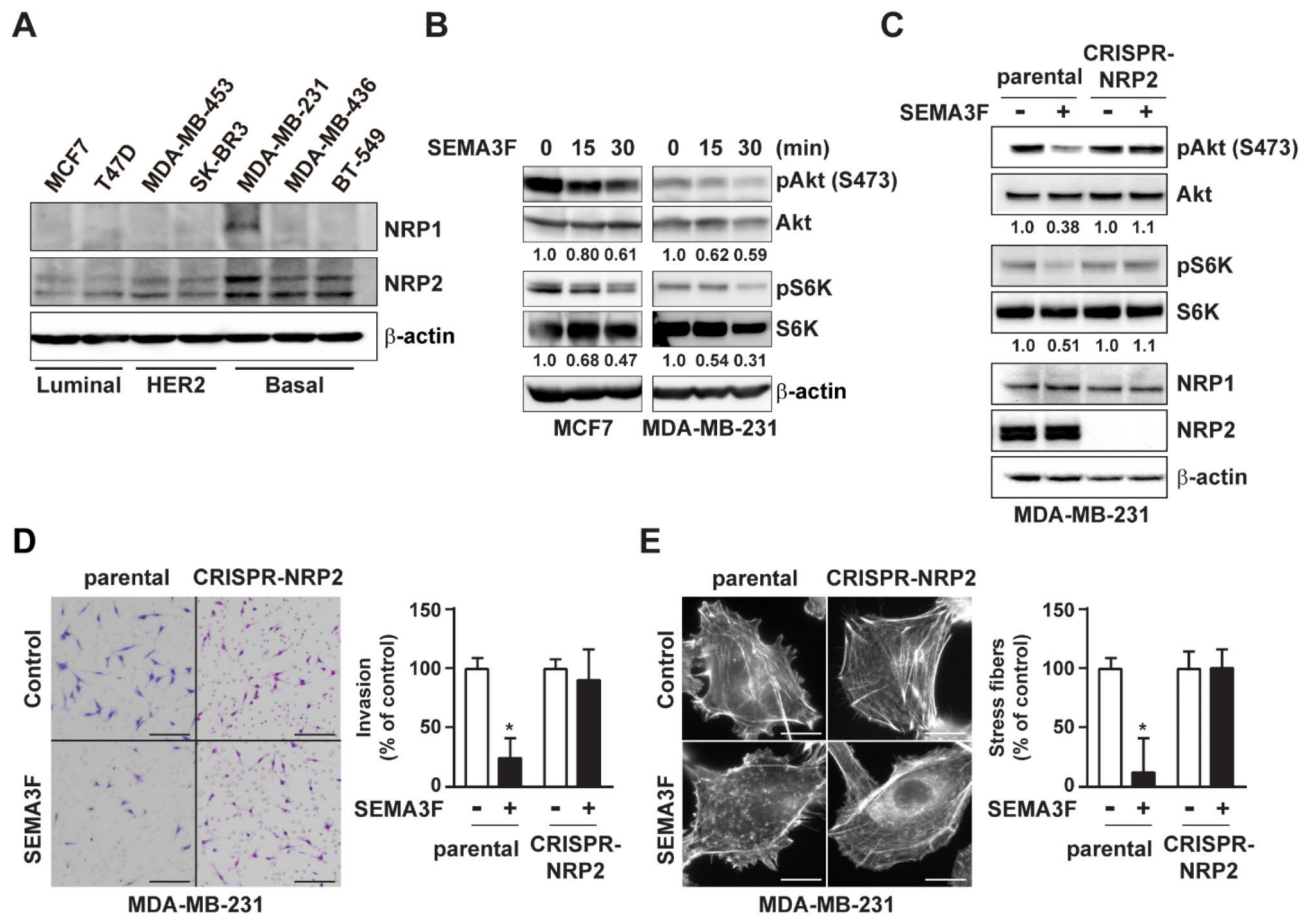


Fig. 2. SEMA3F inhibits Akt and S6K phosphorylation and inactivates invasiveness in breast cancer cells. **(A)** NRP1 and NRP2 receptor protein expression levels were analyzed by Western blot. **(B)** MCF7 and MDA-MB-231 cells were treated with SEMA3F (1800 ng/ml) as a time course up to 30 min and were analyzed by Western blot. The intensity of phosphorylated Akt and S6K bands was normalized to their respective total Akt and S6K, and the numbers below gel lanes represent the fold-change in intensity relative to untreated control. **(C)** NRP2 knockout (CRISPR-NRP2) cells were generated by using the NRP2-CRISPR-Cas9 vector in MDA-MB-231 cells. Cells were treated with SEMA3F (1800 ng/ml) for 30 min and analyzed by Western blot. The intensity of phosphorylated Akt and S6K bands was normalized to their respective total Akt and S6K, and the numbers below gel lanes represent the fold-change in intensity relative to untreated control. **(D)** Parental or NRP2 knockout MDA-MB-231 cells were treated with the addition of SEMA3F (1800 ng/ml), and assessed for their ability to invade with Matrigel-coated Transwells. The scale bar indicates 100 μ m. **(E)** Parental or NRP2 knockout MDA-MB-231 cells were treated with SEMA3F (1800 ng/ml). After 15 min, cells were fixed and stained with rhodamine phalloidin, and observed by fluorescent microscopy. The scale bar indicates 20 μ m. Data represent the mean \pm SD ($n=3$), * $p<0.05$.

performed. 4T1-SEMA3F tumors had a minor area of Ki67 positive cells, compared to control tumors (Fig. 4D). Immunostaining of CD31 revealed fewer blood vessels in 4T1-SEMA3F tumors, whereas there were abundant CD31 positive EC in control 4T1 tumors (Fig. 4D). In addition, 4T1-SEMA3F tumors displayed fewer vimentin positive cells by immunostaining than control tumors (Fig. 4E). Furthermore, by Western blot analysis, we found that phosphorylation of Akt, mTOR, and S6K was suppressed in 4T1-SEMA3F tumors, as compared to controls (Fig. 4F). As 4T1 cells are highly metastatic, we investigated the presence of metastases in the liver and lungs of tumor bearing mice at the end of the experiments, shown in Fig. 4C. We observed that mice implanted with 4T1-Control cells showed metastatic nodules in both the liver and lungs (Fig. 4G). However, in mice implanted with 4T1-SEMA3F cells, the number of metastatic nodules was significantly reduced (Fig. 4G).

We also evaluated the effect of SEMA3F on the human breast cancer cell line, MDA-MB-231, in a xenograft mouse model. The luciferase (Luc)-labeled MDA-MB-231 cells (Luc-MDA-MB-231-Control) and human SEMA3F-V5 stable clones (Luc-MDA-MB-231-SEMA3F) were prepared (Fig. 5A). Initially, we injected Luc-MDA-MB-231-Control or -SEMA3F cells into the mammary fat pads of nude mice (1×10^6 /mouse), and tumor size was measured at the indicated time points over a period of 63 days. In contrast to 4T1 tumor (Fig. 4), there were no significant primary tumor growth differences between controls and SEMA3F tumors either by visual or bioluminescence methods (Fig. 5A-C). In our second approach, we further investigated whether SEMA3F inhibits breast cancer metastasis formation in a mouse tail vein injection tumor metastasis model^{27,28}.

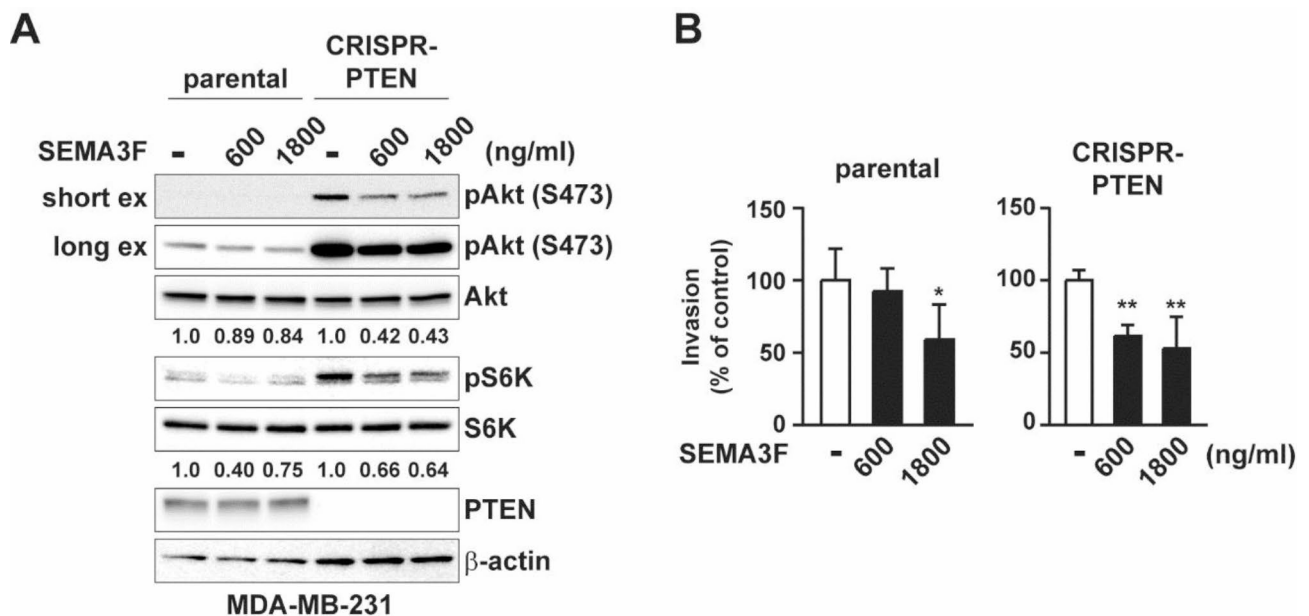


Fig. 3. Effect of SEMA3F on PTEN knockout breast cancer cell. **(A)** PTEN knockout (CRISPR-PTEN) cells were generated by using the PTEN-CRISPR-Cas9 vector in MDA-MB-231 cells. Cells were treated with SEMA3F (1800 ng/ml) for 30 min and analyzed by Western blot. The intensity of phosphorylated Akt and S6K bands was normalized to their respective total Akt and S6K, and the numbers below gel lanes represent the fold-change in intensity relative to untreated control. **(B)** Parental or PTEN knockout MDA-MB-231 cells were treated with the addition of SEMA3F (1800 ng/ml), and assessed for their ability to invade with Matrigel-coated Transwells. Data represent the mean \pm SD ($n = 3$), * $p < 0.05$, ** $p < 0.01$.

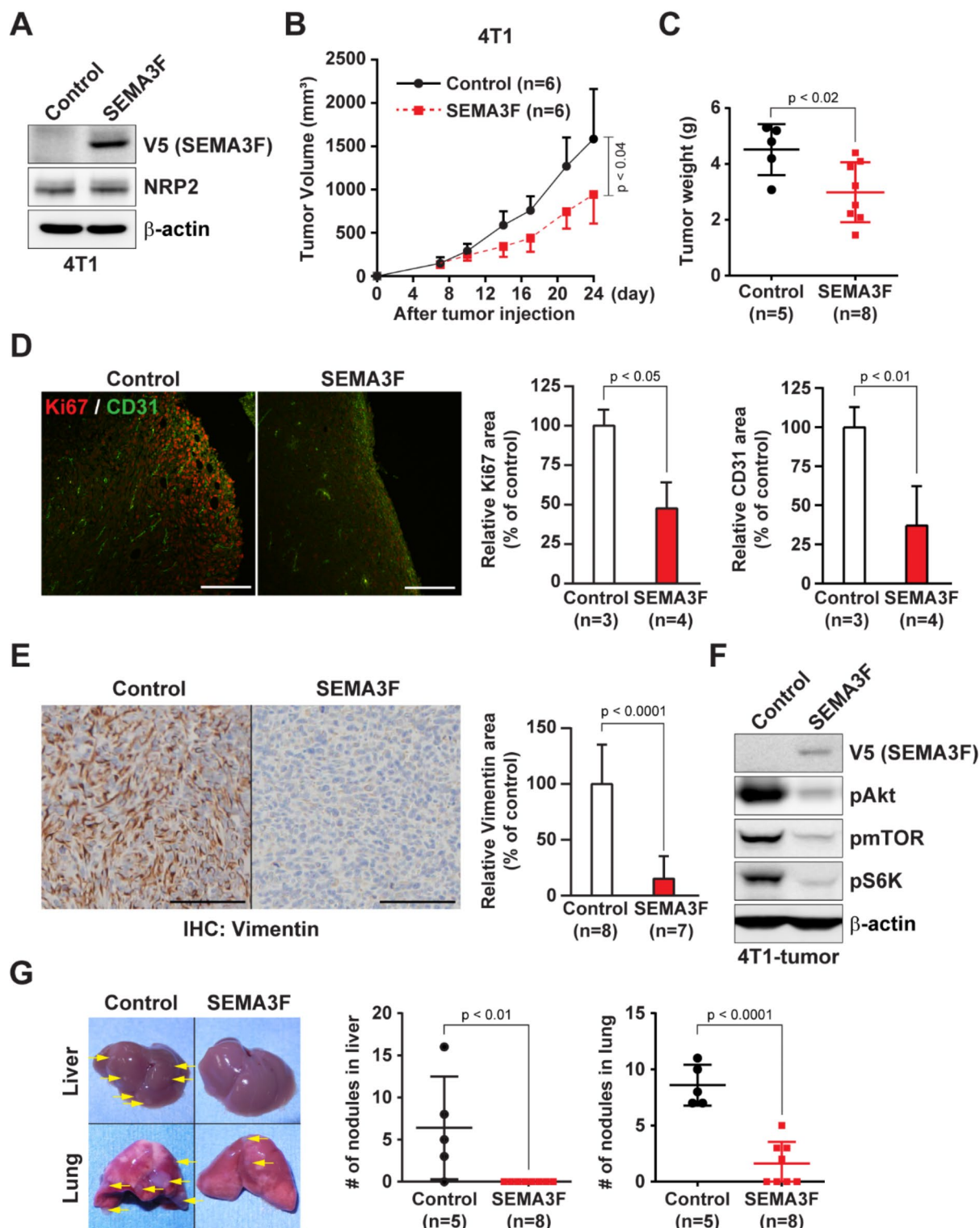
Examination of the lungs using bioluminescence method revealed a significant reduction in metastatic Luc-MDA-MB-231-SEMA3F cells (Fig. 5D). Histological analysis confirmed lung metastasis in the mice injected with Luc-MDA-MB-231-Control cells (Fig. 5E), suggesting that SEMA3F suppresses extravasation potential of MDA-MB-231 cells. Taken together, the marked inhibition of metastasis obtained by two different *in vivo* approaches confirmed that SEMA3F is a potent inhibitor of breast cancer metastasis.

SEMA3F inhibits TGF β signaling via NRP2 in breast cancer cells

Gene expression analysis was performed to investigate the molecular mechanisms underlying SEMA3F activity using the Luc-MDA-MB-231-Control or -SEMA3F cells shown in Fig. 5. Microarray analysis showed that the expression of 26 genes was up-regulated by at least 2.5-fold, and 55 genes were down-regulated by at least 2.5-fold in Luc-MDA-MB-231-SEMA3F cells compared to control cells (Fig. 6A). We found that SEMA3F altered the expression of genes involved in the TGF β signaling pathway. Quantitative real-time polymerase chain reaction (qRT-PCR) experiments confirmed the down-regulation of *TGFBI* (Transforming Growth Factor Beta Induced), *SERPINE1* (Serpin Family E Member 1), *ITGB6* (Integrin Beta 6) by SEMA3F and up-regulation of *SMAD6* in Luc-MDA-MB-231-SEMA3F cells (Fig. 6B). It is well known that breast cancer cells acquire their ability to invade through the TGF β -induced EMT^{5,6}. We found that SEMA3F overexpression led to significant down-regulation of *FN1* (Fibronectin 1), *SNAIL*, and *VIM* (Vimentin), and up-regulation of *CDH1* (Cadherin 1) (Fig. 6C). SEMA3F also suppressed the expression of genes related to TGF β signaling and EMT in PTEN knockout MDA-MB-231 cells (Supplementary Fig. 1D). Because NRP2 acts as a TGF β co-receptor in tumor cells^{15,16}, we investigated whether SEMA3F modulates TGF β signaling in breast cancer cells. SEMA3F suppressed the TGF β -induced Smad2 phosphorylation in MDA-MB-231 cells (Fig. 6D). On the other hand, in NRP2 knockout cells, SEMA3F failed to inhibit Smad2 phosphorylation by TGF β (Fig. 6D). Consistently, SEMA3F blocked TGF β -induced MDA-MB-231 cell invasion, whereas there was no significant difference in NRP2 knockout cells (Fig. 6E). Moreover, TGF β receptor kinase inhibitor, SB431542, inhibited TGF β -induced Smad2 phosphorylation and cell invasion in both parental and NRP2 knockout cells (Supplementary Fig. 2A, B). Together, these results show that SEMA3F inhibits TGF β signaling via NRP2 in breast cancer cells.

Discussion

The *SEMA3F* gene was originally isolated from small cell lung cancer cell lines with a homozygous deletion on chromosome 3p21.3^{29,30}. SEMA3F is markedly down-regulated in highly metastatic human cell lines, including prostate, bladder, and melanoma, *in vitro* and *in vivo*¹⁹. In addition to the exogenously administered SEMA3F, overexpression of SEMA3F in tumor cells, such as lung, colon, and head and neck squamous cell carcinoma cells, has been previously reported to inhibit tumor development and angiogenesis in xenograft mouse models^{31–35}. Based on these studies, it has been suggested that SEMA3F may be a metastasis inhibitor; however, the functional role of SEMA3F in breast cancer is not fully understood. In this study, exogenous addition of SEMA3F inhibited



breast cancer cell invasion through Matrigel *in vitro*, and reduced breast cancer proliferation, angiogenesis, and metastasis *in vivo*. We found that this effect is mediated through the inhibition of Akt-mTOR signaling via NRP2 receptor in breast cancer cells. We also found that SEMA3F inhibited TGFβ signaling via NRP2, resulting in the inhibition of cell invasion and EMT in breast cancer. Our findings suggest that SEMA3F acts as a dual inhibitor of the Akt-mTOR and TGFβ signaling pathways; thus, it has potential to treat metastatic breast cancer. Schematic SEMA3F signaling pathways are described in Fig. 7.

While semaphorins regulate multiple intracellular signaling pathways^{8,36}, a common feature is the modulation of the mTOR pathway^{21,37,38}. mTOR forms two distinct multiprotein complexes, mTORC1 and mTORC2, which are distinguished by their unique accessory proteins, raptor and rictor, respectively³⁹. mTORC1 controls cell growth by regulating protein translation⁴⁰. mTORC2 is involved in actin cytoskeleton reorganization and cell survival⁴¹. The mTOR pathway is implicated in several pathological conditions such as cancer. There is great

Fig. 4. SEMA3F inhibits breast cancer growth, angiogenesis, and metastasis *in vivo*. (A) Western blot analysis of SEMA3F-V5 and NRP2 receptor expression in the 4T1-Control (empty vector) cells and human SEMA3F-V5 stable clones (4T1-SEMA3F). (B) Each cell line was implanted into mammary fat pads of Balb/c mice (1×10^6 cells/injection). Tumor size was measured using a standard calipers at the indicated time points. (C) Tumor weight was measured at the end of experiments. (D) Representative immunohistochemical anti-Ki67 (red) and CD31 (green) staining of tumors harvested after 24 days. The scale bar indicates 100 μ m. The area of Ki67 or CD31 positive cell was measured by ImageJ software. (E) Representative H&E staining and immunohistochemical anti-Vimentin staining of 4T1 tumor harvested after 24 days. The scale bar indicates 200 μ m. The vimentin positive area was measured by ImageJ software. (F) Western blot analysis of the Akt-mTOR signaling pathway within 4T1 tumor samples. (G) Observational analysis of breast cancer cell liver and lung metastases. Arrowheads indicate tumors. The tumor nodules of liver and lung surface per mouse were counted. Numbers in parentheses represent the number of animals in each group. Data represent the mean \pm SD.

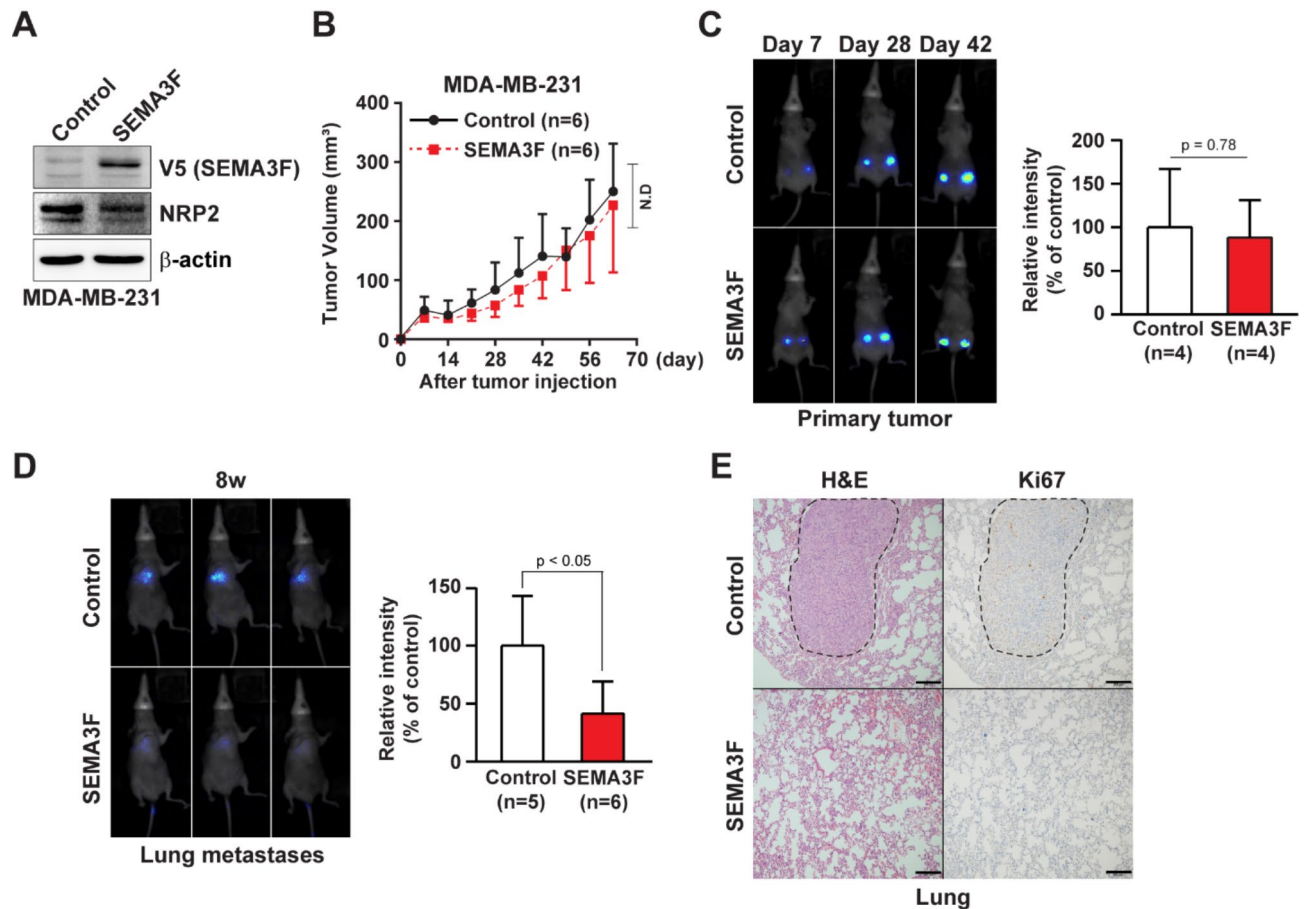


Fig. 5. SEMA3F inhibits human breast cancer metastasis in xenografts *in vivo*. (A) Western blot analysis of SEMA3F-V5 and NRP2 receptor expression in the Luc-labeled MDA-MB-231 cells (Luc-MDA-MB-231-Control) and human SEMA3F-V5 stable clones (Luc-MDA-MB-231-SEMA3F). (B) Each cell line was implanted into mammary fat pads of nude mice (1×10^6 cells/injection). Tumor size was measured using a standard calipers at the indicated time points. (C) Representative bioluminescence images of the indicated Luc-MDA-MB-231 cell lines. The color intensity was analyzed by ImageJ software. (D) Luc-MDA-MB-231-Control or -SEMA3F cells were injected into tail vein of nude mice (1×10^6 cells/injection). Representative bioluminescence images of the indicated Luc-MDA-MB-231 cell lines. The color intensity was analyzed by ImageJ software. (E) Staining for Ki67 identified MDA-MB-231 cells that had metastasized to the lungs harvested after 8 weeks (see areas enclosed by black dotted lines). The scale bar indicates 200 μ m. Numbers in parentheses represent the number of animals in each group. Data represent the mean \pm SD.

interest in early clinical trials of breast cancer therapeutic agents that block multiple points in the PI3K-Akt-mTOR pathway and negative feedback loops associated with reduced clinical efficacy^{42,43}. Since activation of the PI3K-Akt-mTOR pathway is common in breast cancer, we tested the effect of SEMA3F on intracellular signaling pathways. Indeed, we found that SEMA3F inactivated Akt-mTOR signaling in two different human

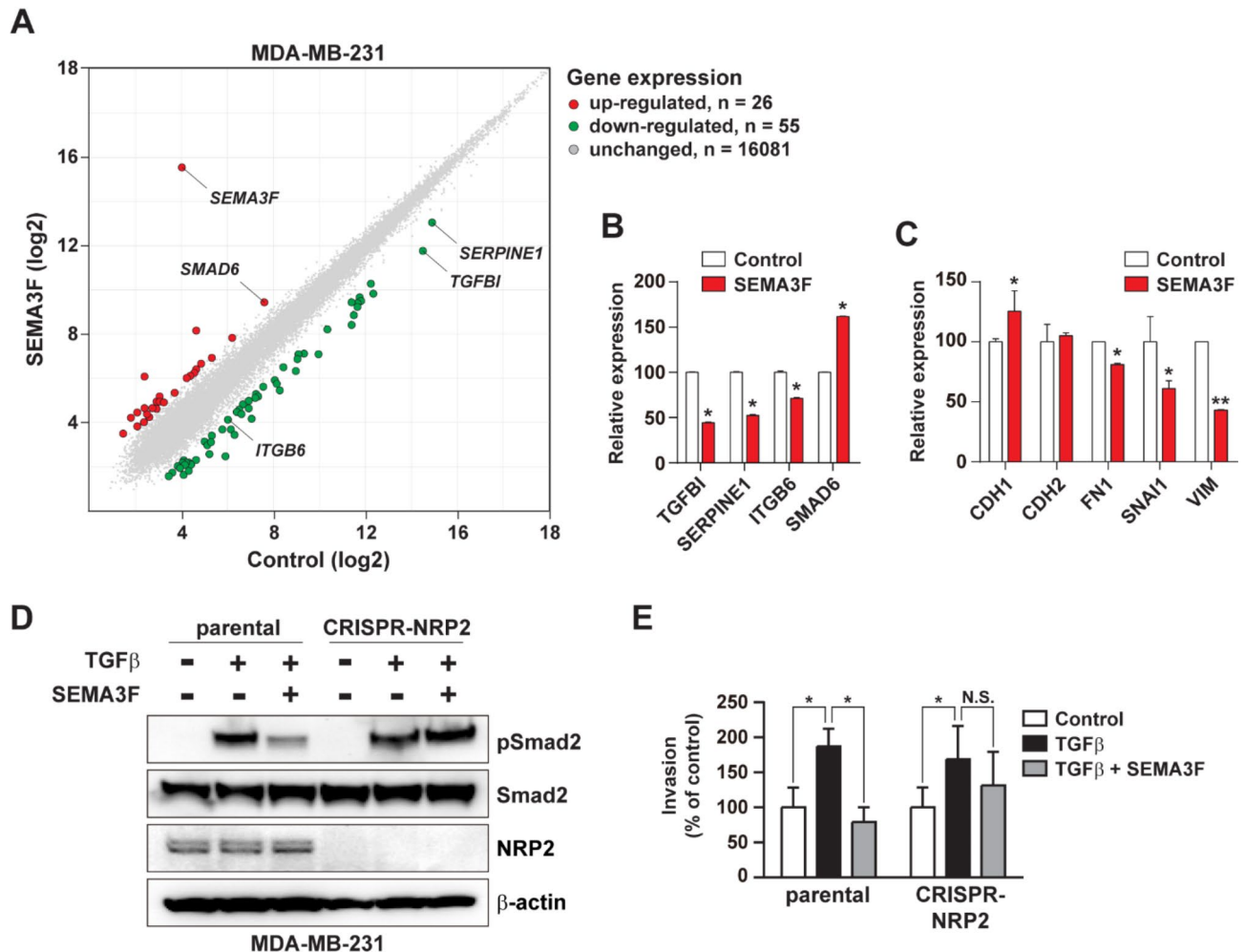


Fig. 6. SEMA3F inhibits TGFβ signaling and EMT in breast cancer cells. **(A)** Microarray-based fold expression of target genes in Luc-MDA-MB-231-SEMA3F cells compared to Luc-MDA-MB-231-Control cells. **(B,C)** Results of the array were validated by qRT-PCR analysis. The bar graphs represent the fold change in each mRNA expression relative to Luc-MDA-MB-231-Control cells. **(D)** Parental or NRP2 knockout MDA-MB-231 cells were pre-treated with SEMA3F (1800 ng/ml) for 15 min and subsequently TGFβ (5 ng/ml) was added to the culture for 15 min. Cells were analyzed by Western blot. **(E)** Parental or NRP2 knockout MDA-MB-231 cells were treated with the addition of TGFβ (5 ng/ml) and/or SEMA3F (1800 ng/ml), and assessed for their ability to invade with Matrigel-coated Transwells. Data represent the mean ± SD (n = 3), * p < 0.05, ** p < 0.01.

breast cancer cell lines as previously described in human lung cancer and glioblastoma cells^{21,44}. In addition, we found that phosphorylation of Akt, mTOR, and S6K was suppressed in 4T1-SEMA3F tumors compared to controls, which is consistent with its effects *in vitro*. The collapsing activity of SEMA3F has been reported to be mediated by the disruption of mTOR/ricor assembly (mTORC2 activity) and inhibition of RhoA signaling^{20,21}. SEMA3F suppresses hypoxia-induced VEGF-A production via the mTOR pathway²¹. These molecular results in response to SEMA3F are compatible with reduced angiogenic and metastatic activities of breast cancer *in vivo*.

Inactivation or loss of PTEN, a negative regulator of PI3K, occurs commonly in breast cancer and can lead to the activation of the PI3K-Akt-mTOR pathway^{25,26}. It has been reported that NRP1 interacts with PTEN on its cytoplasmic domain consisting of a PDZ domain binding motif (carboxy-terminal amino acid sequence: Ser-Glu-Ala). SEMA4A-NRP1 interactions recruit PTEN and attenuate Akt-mTOR signaling in regulatory T cells⁴⁵. Consistently, PTEN interacts with NRP2 in human umbilical vein EC (HUVEC), suggesting that SEMA3F-NRP2 interactions inhibit Akt-mTOR signaling by recruiting PTEN to regulate PI3K^{13,21}. However, SEMA3F inhibited Akt-mTOR signaling and invasive activity in PTEN knockout breast cancer cells. We also noted that SEMA3F suppressed the expression of genes related to TGFβ signaling and EMT in PTEN knockout cells. Thus, we suggest that SEMA3F may also elicit regulatory response(s) via PTEN-independent mechanisms in breast cancer cell. The additional adaptors/kinases may also function in the SEMA3F-mediated responses. Loss of PTEN is associated with aggressive breast cancer and worse outcomes for patients^{25,26}. Therefore, SEMA3F-NRP2 interactions could be a target to repress the invasive activity of PTEN loss breast cancer.

A novel aspect of our study is that SEMA3F inhibits the TGFβ-induced cell activation and EMT in breast cancer cells. TGFβ is a potent inducer of EMT and plays an important role in embryonic development and

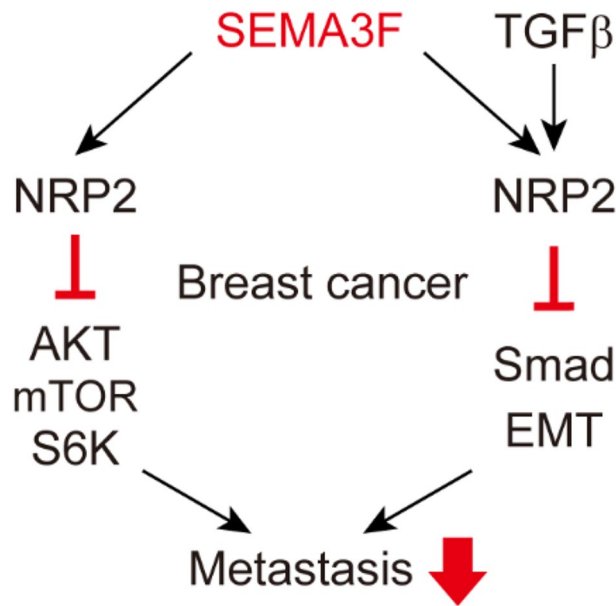


Fig. 7. Schematic of SEMA3F-dependent pathways. SEMA3F inactivates Akt and mTOR downstream signaling molecules, including S6K, via NRP2 in breast cancer cells. SEMA3F also inhibits TGFβ-induced phosphorylation of Smad2, thereby inhibiting breast cancer cell invasion and EMT. Our findings suggest that SEMA3F acts as a dual inhibitor of the Akt-mTOR and TGFβ signaling pathways, indicating its potential for the inhibition of breast cancer metastasis.

transformation of early stage tumors into invasive malignancies^{5,6}. NRP1 acts as a TGFβ co-receptor and activates latent TGFβ in breast cancer⁴⁶. NRP2 also binds to TGFβ and induces TGFβ-mediated EMT in colorectal cancer and lung cancer cells^{15,16}. In this study, we found that SEMA3F inhibited TGFβ-induced Smad2 activation and invasiveness via NRP2 receptor in MDA-MB-231 cells. Previous report showed that a direct binding activity of NRP2 for TGFβ, leading to cooperation with TGFRI and subsequent Smad2/3 phosphorylation¹⁵. This may suggest that SEMA3F inhibits NRP2-TGFβRI interaction in response to TGFβ, or SEMA3F interferes with TGFβ binding to NRP2 because of overlapping binding sites in the extracellular domain of NRP2^{15,47}. Alternatively, it is possible that SEMA3F-NRP2 interaction may inactivate Smad2 via TGFβRI/II-independent mechanisms in breast cancer cells. Further work is needed to dissect the mechanisms underlying the inhibitory effects of SEMA3F on TGFβ signaling. Nevertheless, our results provide the evidence that SEMA3F, a soluble ligand for NRP2 receptor, modulates TGFβ signaling, suggesting new perspectives to design specific targeted therapeutics.

Our *in vitro* and *in vivo* results are compatible with the clinical data of patients with metastatic breast cancer showing significant reductions in SEMA3F expression in tumor samples. These results may be of clinical significance. However, while SEMA3F inhibited growth of 4T1 cells in fat pads of Balb/c mice (Fig. 4), it had no inhibitory effect on MDA-MB-231 cells in fat pads of nude mice (Fig. 5). These inconsistent results might be a result of the compromised immune system or the limited cross-species activity between mice and human. Mouse experimental models do not entirely resemble human breast cancer characteristics, such as gene regulation, immune response, or metastatic behavior. This may limit the translational prospective of the study. To improve our findings, the existing alternative models, such as patient-derived xenograft or humanized mouse models, are better to replicate human breast cancer.

In conclusion, our data implicate SEMA3F as a potent inhibitor of metastatic activity in breast cancer via the suppression of both Akt-mTOR and TGFβ signaling pathways. Breast cancer metastasis is a major cause of cancer-related death. This poor prognosis stems largely from the highly invasive nature of breast cancer, which makes therapy extremely challenging. We conclude that these results identify SEMA3F as a potential new target for the treatment of aggressive breast cancer.

Methods

Antibodies and reagents

The antibodies, mouse monoclonal anti-phospho-Akt (Ser473) antibody (#4051); rabbit polyclonal anti-Akt antibody (#9272); rabbit monoclonal anti-phospho-S6K (Thr389) antibody (#9234); rabbit monoclonal anti-S6K antibody (#2708); rabbit monoclonal anti-phospho-Smad2 antibody (#3108); rabbit monoclonal anti-Smad2 antibody (#5339); rabbit monoclonal anti-PTEN antibody (#9188); rabbit monoclonal anti-vimentin antibody (#5741); rabbit monoclonal anti-NRP2 (#3366) were all purchased from Cell Signaling Technology. Mouse monoclonal anti-NRP1 antibody (A-12, sc-5307) and mouse monoclonal anti-NRP2 antibody (C-9, sc-13117); were purchased from Santa Cruz Biotechnology, Inc. Mouse monoclonal anti-V5 tag antibody (#46-0705) and mouse monoclonal anti-β-actin antibody (AC-15) were purchased from Invitrogen and Sigma-Aldrich, respectively. Rat monoclonal anti-CD31 antibody (SZ31) and rabbit monoclonal anti-Ki67 antibody

(ab16667) were obtained from Dianova and Abcam, respectively. The recombinant human TGF β 1 (#240-B) and the TGF β receptor kinase inhibitor, SB431542 were purchased from R&D Systems and Wako, respectively.

Cell culture

The human and mouse breast cancer cells were supplied by the American Type Culture Collection. MDA-MB-231 (#HTB-26), 436 (#HTB-130), and 453 (#HTB-131) cells were cultured in Leibovitz's L-15 Medium supplemented with 10% fetal bovine serum (FBS, Wako) in atmospheric air at 37 °C. SKBR3 cells (#HTB-30) were cultured in Dulbecco's Modified Eagle Medium (DMEM) supplemented with 10% FBS. T47D (#HTB-133) and BT549 (#HTB-122) cells were cultured in RPMI1640 medium supplemented with 10% FBS and insulin (0.01 mg/ml). MCF7 cells (#HTB-22) were cultured in Eagle's Minimum Essential Medium (EMEM) supplemented with 10% FBS and insulin (0.01 mg/ml). Mouse breast cancer cells 4T1 (#CRL-2539) were cultured in RPMI1640 medium supplemented with 10% FBS. Cells were maintained in a humidified incubator at 37 °C/5% CO₂ incubator.

The human SEMA3F and luciferase (stable luciferase red, Toyobo) were expressed using a lentiviral system⁴⁸. The cDNA fragments of V5-tagged human SEMA3F (SEMA3F-V5) or luciferase (Luc) were subcloned into the lentiviral expression vector, CSII-EF-MCS-IRES2-Bsd or CSII-EF-MCS-IRES2-Puro, respectively. An empty lentiviral vector (Control) was used as a negative control. Each lentiviral expression vector was transfected into 293T cells together with two packaging plasmids, pCAG-HIVgp and pCMV-VSV-G-RSV-Rev. 4T1 and MDA-MB-231 cells were infected with Control- or SEMA3F-expressing lentiviruses and the infected cells were maintained in the presence of blasticidin. MDA-MB-231-Control and -SEMA3F cells were infected with Luc-expressing lentiviruses and the infected cells were maintained in the presence of blasticidin and puromycin. Each pool of infected cells resistant to blasticidin and/or puromycin was used in experiments.

Analysis of publicly available datasets

The correlation between relapse-free survival (RSF) of breast cancer patients and SEMA3F expression was analyzed using the Kaplan-Meier plotter (<http://kmplot.com/analysis/>)^{22–24}.

CRISPR/Cas9 and selection

Guide RNA targeting NRP2 (GTAGAGGGCTAAGAAAACCC) or PTEN (TGGGAATAGTTACTCCCTG G) was ligated into the lentiCRISPR v2 (Plasmid #52961, Addgene). Lentiviral particles were generated by a standard transfection procedure⁴⁸. After transduction of the transgenes, the pool of MDA-MB-231 cells resistant to puromycin were used in the experiments.

Recombinant SEMA3F protein

A full-length His-Myc-tagged human SEMA3F construct was transfected into 293T cells using FuGENE HD Transfection Reagent (Roche). SEMA3F secreted into the culture medium was purified using HiTrap HP Chelating columns (GE Healthcare)⁴⁹.

Western blotting

Each sample was separated by sodium dodecyl sulfate polyacrylamide gel electrophoresis, and the gels were transferred to nitrocellulose membranes. The membranes were blocked with 4% skim milk in Tris-buffered saline (TBS)-T (0.1% Tween 20 in TBS) for 30 min, followed by incubation with primary antibodies. After washing with TBS-T, the membranes were incubated with appropriate horseradish peroxidase-conjugated secondary antibodies. Immunoreactivity was detected using ECL detection reagents (PerkinElmer).

Invasion assays

Invasion assays were performed in 'Transwells' (Corning Glass) with an 8.0 μ m pore size and coated with BD Matrigel[®] Phenol Red-Free Growth Factor Reduced Basement Membrane Matrix (Ref 356231, BD Biosciences) (0.1 mg/mL). Cells that had migrated through the filters after 16 h at 37 °C were stained with the Diff-Quick cell staining kit (Dade Behring Inc.), and four fields were counted by phase microscopy.

F-actin staining

Cells were fixed with 4% paraformaldehyde (PFA) followed by permeabilization with 0.2% Triton X-100 in PBS. F-actin was stained with rhodamine phalloidin reagent (Abcam). Confocal images from 3 to 5 areas of each culture were reviewed and stress fibers were counted in representative individual cells.

Animal studies

For allograft model, 4T1-Control or 4T1-SEMA3F cells (1×10^6 /injection) were resuspended in an ice-cold 50:50 solution of Matrigel and were orthotopically implanted into the mammary gland of Balb/c mice (female, 4–6 weeks of age, Japan SLC, Inc.). Tumor size was measured every 3–4 days using standard calipers. Mice were sacrificed on day 24, and tumors and tissues were removed. Tumor weight was measured in the different experimental mouse group to confirm reliability of *in vivo* study. Metastatic nodules in the liver and lungs were counted by visual observation. For xenograft model, MDA-MB-231-Luc-Control or MDA-MB-231-Luc-SEMA3F cells were orthotopically implanted into the mammary gland of nude mice (female, 4–6 weeks of age, Japan SLC, Inc.). Tumor size was measured every 3–4 days using standard calipers. Alternatively, tumor growth was assessed using as read out bioluminescence generated by the Luc-expressing cells. Images were captured by AEQUORIA-2D (Hamamatsu Photonics) in 10 min after D-luciferin (Promega) administration via the tail vein. In a second model, MDA-MB-231-Luc-Control or MDA-MB-231-Luc-SEMA3F cells (1×10^6 /injection) were injected via the tail vein. Metastasis of MDA-MB-231 cells was determined by bioluminescence methods as described above. These animal studies were modified from published procedures^{27,28}. CO₂ inhalation was

used for euthanizing for mice. All mice received standard care, and our study protocol was approved by the Ethics Committee of the Graduate School of Medicine, Ehime University, Japan. All methods were carried out in accordance with relevant guidelines and regulations. All procedures were conducted in full compliance with the ARRIVE guidelines.

Immunohistochemistry

Paraffin-embedded sections were deparaffinized and activated in sodium citrate buffer (10mM Sodium Citrate, 0.05% Tween 20, pH 6.0) at 95 °C for 15 min and processed for immunohistochemical staining. Sections were stained with primary antibodies for overnight and the respective secondary antibodies were labeled with Alexa Fluor 488 or 594 (Molecular Probes). Digital images of sections were captured using a confocal laser scanning microscope (A1, Nikon).

Quantitative real-time polymerase chain reaction (qRT-PCR)

Total RNA was isolated using NucleoSpin[®] RNA Plus (Takara Bio Inc.), and reverse transcription of RNA was performed with a high-capacity RNA-to-cDNA kit (Thermo Fisher Scientific) according to the manufacturer's instructions. After first-strand synthesis, qRT-PCR was performed using a FastStart Universal SYBR Green Master (ROX) mixture (Roche) with a 7300 real-time PCR system (Applied Biosystems). The qRT-PCR primers used in this study are listed in Supplementary Table 1. mRNA expression levels were normalized to that of GAPDH.

Microarray analysis

To identify SEMA3F response genes in breast cancer cells, total RNA was isolated from Luc-MDA-MB-231-Control or -SEMA3F cells using NucleoSpin[®] RNA Plus. Biotinylated cDNA was prepared from 100 ng of total RNA using GeneChip WT PLUS Reagent Kit (Thermo Fisher Scientific) following the manufacturer's instructions. Following fragmentation, 2 µg of single-stranded cDNA was hybridized for 16 h at 45 °C on Clariom S Array, Human. The arrays were washed and stained in the GeneChip Fluidics Station 450 (Thermo Fisher Scientific). Clariom S array was scanned using GeneChip Scanner 3000 7G. The data were analyzed with Transcriptome Analysis Console (TAC) 4.0.2 (Thermo Fisher Scientific). Microarray analysis was performed in duplicate.

Statistical analysis

All assays were performed independently at least three times. The results are represented as mean ± standard deviation (SD). The groups were compared using Student's t test, and p values < 0.05 were considered statistically significant.

Data availability

The datasets used and/or analysed during the current study available from the corresponding author on reasonable request.

Received: 16 October 2024; Accepted: 21 February 2025

Published online: 03 March 2025

References

- Sung, H. et al. Global Cancer statistics 2020: GLOBOCAN estimates of incidence and mortality worldwide for 36 cancers in 185 countries. *CA Cancer J. Clin.* **71**, 209–249. <https://doi.org/10.3322/caac.21660> (2021).
- Agus, D. B. et al. Targeting ligand-activated ErbB2 signaling inhibits breast and prostate tumor growth. *Cancer Cell.* **2**, 127–137. [https://doi.org/10.1016/s1535-6108\(02\)00097-1](https://doi.org/10.1016/s1535-6108(02)00097-1) (2002).
- Brüner-Kubath, C. et al. The PI3 kinase/mtor blocker NVP-BEZ235 overrides resistance against irreversible erbb inhibitors in breast cancer cells. *Breast Cancer Res. Treat.* **129**, 387–400. <https://doi.org/10.1007/s10549-010-1232-1> (2011).
- Junttila, T. T. et al. Ligand-independent HER2/HER3/PI3K complex is disrupted by trastuzumab and is effectively inhibited by the PI3K inhibitor GDC-0941. *Cancer Cell.* **15**, 429–440. <https://doi.org/10.1016/j.ccr.2009.03.020> (2009).
- Kang, Y. et al. A Multigenic program mediating breast cancer metastasis to bone. *Cancer Cell.* **3**, 537–549. [https://doi.org/10.1016/s1535-6108\(03\)00132-6](https://doi.org/10.1016/s1535-6108(03)00132-6) (2003).
- Massagué, J. & Sheppard, D. TGF-β signaling in health and disease. *Cell* **186**, 4007–4037. <https://doi.org/10.1016/j.cell.2023.07.036> (2023).
- Bagri, A., Tessier-Lavigne, M. & Watts, R. J. Neuropilins in tumor biology. *Clin. Cancer Res.* **15**, 1860–1864. <https://doi.org/10.1158/1078-0432.Ccr-08-0563> (2009).
- Klagsbrun, M. & Eichmann, A. A role for axon guidance receptors and ligands in blood vessel development and tumor angiogenesis. *Cytokine Growth Factor. Rev.* **16**, 535–548. <https://doi.org/10.1016/j.cytogfr.2005.05.002> (2005).
- Tang, Y. H. et al. Neuropilin-1 is over-expressed in claudin-low breast cancer and promotes tumor progression through acquisition of stem cell characteristics and RAS/MAPK pathway activation. *Breast Cancer Res.* **24**, 8. <https://doi.org/10.1186/s13058-022-01501-7> (2022).
- Yasuoka, H. et al. Neuropilin-2 expression in breast cancer: correlation with lymph node metastasis, poor prognosis, and regulation of CXCR4 expression. *BMC Cancer.* **9**, 220. <https://doi.org/10.1186/1471-2407-9-220> (2009).
- Migdal, M. et al. Neuropilin-1 is a placenta growth factor-2 receptor. *J. Biol. Chem.* **273**, 22272–22278. <https://doi.org/10.1074/jbc.273.35.22272> (1998).
- West, D. C. et al. Interactions of multiple heparin binding growth factors with neuropilin-1 and potentiation of the activity of fibroblast growth factor-2. *J. Biol. Chem.* **280**, 13457–13464. <https://doi.org/10.1074/jbc.M410924200> (2005).
- Gemmell, R. M. et al. The neuropilin 2 isoform NRP2b uniquely supports TGFβ-mediated progression in lung cancer. *Sci. Signal.* **10** <https://doi.org/10.1126/scisignal.aag0528> (2017).
- Sulpice, E. et al. Neuropilin-1 and neuropilin-2 act as coreceptors, potentiating proangiogenic activity. *Blood* **111**, 2036–2045. <https://doi.org/10.1182/blood-2007-04-084269> (2008).

15. Grandclement, C. et al. Neuropilin-2 expression promotes TGF- β 1-mediated epithelial to mesenchymal transition in colorectal cancer cells. *PLoS One*. **6**, e20444. <https://doi.org/10.1371/journal.pone.0020444> (2011).
16. Nasarre, P. et al. Neuropilin-2 is upregulated in lung cancer cells during TGF- β 1-induced epithelial-mesenchymal transition. *Cancer Res.* **73**, 7111–7121. <https://doi.org/10.1158/0008-5472.Can-13-1755> (2013).
17. Giger, R. J. et al. Neuropilin-2 is a receptor for semaphorin IV: insight into the structural basis of receptor function and specificity. *Neuron* **21**, 1079–1092. [https://doi.org/10.1016/s0896-6273\(00\)80625-x](https://doi.org/10.1016/s0896-6273(00)80625-x) (1998).
18. Takahashi, T. & Strittmatter, S. M. PlexinA1 autoinhibition by the Plexin Sema domain. *Neuron* **29**, 429–439. [https://doi.org/10.1016/s0896-6273\(01\)00216-1](https://doi.org/10.1016/s0896-6273(01)00216-1) (2001).
19. Bielenberg, D. R. et al. Semaphorin 3F, a chemorepellant for endothelial cells, induces a poorly vascularized, encapsulated, nonmetastatic tumor phenotype. *J. Clin. Invest.* **114**, 1260–1271. <https://doi.org/10.1172/jci21378> (2004).
20. Shimizu, A. et al. ABL2/ARG tyrosine kinase mediates SEMA3F-induced RhoA inactivation and cytoskeleton collapse in human glioma cells. *J. Biol. Chem.* **283**, 27230–27238. <https://doi.org/10.1074/jbc.M804520200> (2008).
21. Nakayama, H. et al. Regulation of mTOR signaling by semaphorin 3F-Neuropilin 2 interactions in vitro and in vivo. *Sci. Rep.* **5**, 11789. <https://doi.org/10.1038/srep11789> (2015).
22. Györfy, B. et al. An online survival analysis tool to rapidly assess the effect of 22,277 genes on breast cancer prognosis using microarray data of 1,809 patients. *Breast Cancer Res. Treat.* **123**, 725–731. <https://doi.org/10.1007/s10549-009-0674-9> (2010).
23. Lánckzy, A. & Györfy, B. Web-Based survival analysis tool tailored for medical research (KMplot): development and implementation. *J. Med. Internet Res.* **23**, e27633. <https://doi.org/10.2196/27633> (2021).
24. Györfy, B. Survival analysis across the entire transcriptome identifies biomarkers with the highest prognostic power in breast cancer. *Comput. Struct. Biotechnol. J.* **19**, 4101–4109. <https://doi.org/10.1016/j.csbj.2021.07.014> (2021).
25. Nagata, Y. et al. PTEN activation contributes to tumor inhibition by trastuzumab, and loss of PTEN predicts trastuzumab resistance in patients. *Cancer Cell*. **6**, 117–127. <https://doi.org/10.1016/j.ccr.2004.06.022> (2004).
26. Pandolfi, P. P. Breast cancer—loss of PTEN predicts resistance to treatment. *N Engl. J. Med.* **351**, 2337–2338. <https://doi.org/10.1056/NEJMcibr043143> (2004).
27. Fitamant, J. et al. Netrin-1 expression confers a selective advantage for tumor cell survival in metastatic breast cancer. *Proc. Natl. Acad. Sci. U S A*. **105**, 4850–4855. <https://doi.org/10.1073/pnas.0709810105> (2008).
28. Morris, D. C. et al. Nck deficiency is associated with delayed breast carcinoma progression and reduced metastasis. *Mol. Biol. Cell*. **28**, 3500–3516. <https://doi.org/10.1091/mbc.E17-02-0106> (2017).
29. Roche, J. et al. Distinct 3p21.3 deletions in lung cancer and identification of a new human semaphorin. *Oncogene* **12**, 1289–1297 (1996).
30. Sekido, Y. et al. Human semaphorins A(V) and IV reside in the 3p21.3 small cell lung cancer deletion region and demonstrate distinct expression patterns. *Proc. Natl. Acad. Sci. U S A*. **93**, 4120–4125. <https://doi.org/10.1073/pnas.93.9.4120> (1996).
31. Bollard, J. et al. The axon guidance molecule semaphorin 3F is a negative regulator of tumor progression and proliferation in ileal neuroendocrine tumors. *Oncotarget* **6**, 36731–36745. <https://doi.org/10.18632/oncotarget.5481> (2015).
32. Doçi, C. L., Mikelis, C. M., Lionakis, M. S., Molinolo, A. A. & Gutkind, J. S. Genetic identification of SEMA3F as an antilymphangiogenic metastasis suppressor gene in head and neck squamous carcinoma. *Cancer Res.* **75**, 2937–2948. <https://doi.org/10.1158/0008-5472.Can-14-3121> (2015).
33. Futamura, M. et al. Possible role of semaphorin 3F, a candidate tumor suppressor gene at 3p21.3, in p53-regulated tumor angiogenesis suppression. *Cancer Res.* **67**, 1451–1460. <https://doi.org/10.1158/0008-5472.Can-06-2485> (2007).
34. Kigel, B., Varshavsky, A., Kessler, O. & Neufeld, G. Successful inhibition of tumor development by specific class-3 semaphorins is associated with expression of appropriate semaphorin receptors by tumor cells. *PLoS One*. **3**, e3287. <https://doi.org/10.1371/journal.pone.0003287> (2008).
35. Wu, F. et al. Endogenous axon guiding chemorepellant semaphorin-3F inhibits the growth and metastasis of colorectal carcinoma. *Clin. Cancer Res.* **17**, 2702–2711. <https://doi.org/10.1158/1078-0432.Ccr-10-0839> (2011).
36. Neufeld, G. & Kessler, O. The semaphorins: versatile regulators of tumour progression and tumour angiogenesis. *Nat. Rev. Cancer*. **8**, 632–645. <https://doi.org/10.1038/nrc2404> (2008).
37. Nakanishi, Y., Kang, S. & Kumanogoh, A. Neural guidance factors as hubs of immunometabolic cross-talk. *Int. Immunol.* **33**, 749–754. <https://doi.org/10.1093/intimm/dxab035> (2021).
38. Nukazuka, A. et al. A shift of the TOR adaptor from rictor towards raptor by semaphorin in *C. elegans*. *Nat. Commun.* **2**, 484. <https://doi.org/10.1038/ncomms1495> (2011).
39. Saxton, R. A. & Sabatini, D. M. mTOR signaling in growth, metabolism, and disease. *Cell* **168**, 960–976. <https://doi.org/10.1016/j.cell.2017.02.004> (2017).
40. Kim, D. H. et al. mTOR interacts with raptor to form a nutrient-sensitive complex that signals to the cell growth machinery. *Cell* **110**, 163–175. [https://doi.org/10.1016/s0092-8674\(02\)00808-5](https://doi.org/10.1016/s0092-8674(02)00808-5) (2002).
41. Huang, W. et al. mTORC2 controls actin polymerization required for consolidation of long-term memory. *Nat. Neurosci.* **16**, 441–448. <https://doi.org/10.1038/nn.3351> (2013).
42. O'Reilly, K. E. et al. mTOR inhibition induces upstream receptor tyrosine kinase signaling and activates Akt. *Cancer Res.* **66**, 1500–1508. <https://doi.org/10.1158/0008-5472.Can-05-2925> (2006).
43. Zoncu, R., Efeyan, A. & Sabatini, D. M. mTOR: from growth signal integration to cancer, diabetes and ageing. *Nat. Rev. Mol. Cell Biol.* **12**, 21–35. <https://doi.org/10.1038/nrm3025> (2011).
44. Potiron, V. A. et al. Semaphorin SEMA3F affects multiple signaling pathways in lung cancer cells. *Cancer Res.* **67**, 8708–8715. <https://doi.org/10.1158/0008-5472.Can-06-3612> (2007).
45. Delgoffe, G. M. et al. Stability and function of regulatory T cells is maintained by a neuropilin-1-semaphorin-4a axis. *Nature* **501**, 252–256. <https://doi.org/10.1038/nature12428> (2013).
46. Glinka, Y., Stoilova, S., Mohammed, N. & Prud'homme, G. J. Neuropilin-1 exerts co-receptor function for TGF- β 1 on the membrane of cancer cells and enhances responses to both latent and active TGF- β . *Carcinogenesis* **32**, 613–621. <https://doi.org/10.1093/carcin/bgq281> (2011).
47. Pawlak, J. B. & Blobel, G. C. TGF- β superfamily co-receptors in cancer. *Dev. Dyn.* **251**, 137–163. <https://doi.org/10.1002/dvdy.338> (2022).
48. Miyoshi, H., Blömer, U., Takahashi, M., Gage, F. H. & Verma, I. M. Development of a self-inactivating lentivirus vector. *J. Virol.* **72**, 8150–8157. <https://doi.org/10.1128/jvi.72.10.8150-8157.1998> (1998).
49. Bielenberg, D. R., Shimizu, A. & Klagsbrun, M. Semaphorin-induced cytoskeletal collapse and repulsion of endothelial cells. *Methods Enzymol.* **443**, 299–314. [https://doi.org/10.1016/s0076-6879\(08\)02015-6](https://doi.org/10.1016/s0076-6879(08)02015-6) (2008).

Acknowledgements

Research reported in this publication was supported in part by Japan Society for the Promotion of Science (JSPS) KAKENHI Grant Numbers 18K08984, 21K09192 (H.N.), and 17K10553 (Y.K.). This study was supported by Ehime University Proteo-Science Center (PROS) and Advanced Research Support Center. We thank Dr. Yuuki Imai (PROS, Ehime University) for technical support of animal experiment.

Author contributions

Conception and design: H.N, S.F, C.K, Y.M, S.H; Acquisition of data: H.N, A.M, H.F, E.M, M.N; Analysis and interpretation of data: H.N, H.F, S.F, S.H; Writing and review: H.N, H.F, S.F, S.H.

Declarations

Competing interests

The authors declare no competing interests.

Additional information

Supplementary Information The online version contains supplementary material available at <https://doi.org/10.1038/s41598-025-91559-y>.

Correspondence and requests for materials should be addressed to H.N. or S.H.

Reprints and permissions information is available at www.nature.com/reprints.

Publisher's note Springer Nature remains neutral with regard to jurisdictional claims in published maps and institutional affiliations.

Open Access This article is licensed under a Creative Commons Attribution-NonCommercial-NoDerivatives 4.0 International License, which permits any non-commercial use, sharing, distribution and reproduction in any medium or format, as long as you give appropriate credit to the original author(s) and the source, provide a link to the Creative Commons licence, and indicate if you modified the licensed material. You do not have permission under this licence to share adapted material derived from this article or parts of it. The images or other third party material in this article are included in the article's Creative Commons licence, unless indicated otherwise in a credit line to the material. If material is not included in the article's Creative Commons licence and your intended use is not permitted by statutory regulation or exceeds the permitted use, you will need to obtain permission directly from the copyright holder. To view a copy of this licence, visit <http://creativecommons.org/licenses/by-nc-nd/4.0/>.

© The Author(s) 2025